Kinetics of Carbamylcholine Binding to Membrane-Bound Acetylcholine Receptor Monitored by Fluorescence Changes of a Covalently Bound Probe†

Susan M. J. Dunn, Steven G. Blanchard, and Michael A. Raftery*

ABSTRACT: The fluorescent probe 5-(iodoacetamido)salicylic acid has been used to alkylate acetylcholine receptor enriched membrane fragments from *Torpedo californica* following their reduction with low concentrations of dithiothreitol. This modification did not affect the equilibrium binding of carbamylcholine to the receptor. The fluorescence of bound 5-(iodoacetamido)salicylic acid was enhanced when the labeled membrane fragments were mixed with carbamylcholine. This increase in fluorescence was abolished by preincubation of the membrane fragments with excess α-bungarotoxin and was therefore specific for the acetylcholine receptor. Estimates of dissociation constants obtained from centrifugation experiments with radioactive ligand and from fluorescence titration data were in good agreement, showing that the observed fluorescence enhancement was an accurate reflection of receptor–carbamylcholine complex formation. The kinetics of carbamylcholine binding to labeled membrane fragments have been investigated over a wide range of ligand concentrations by using stopped-flow fluorescence techniques. The kinetic signal was complicated, and four distinct exponential phases were observed. A kinetic mechanism has been proposed to account for this behavior.

Acetylcholine receptor (AcChR)[1] enriched membrane fragments prepared from *Torpedo* electric organs have been extensively used for in vitro studies of the ligand binding and functional properties of the nicotinic receptor in its membrane environment.

The kinetics of ligand binding to AcChR preparations have been studied by rapid-mixing experiments in which various fluorescence techniques have been used to monitor complex formation and consequent conformational changes. The effect of AcCh binding on the intrinsic fluorescence of membrane-bound AcChR has been described (Bonner et al., 1976; Barrantes, 1976). Although this is the most direct method, it lacks sensitivity due to the weak fluorescence of the receptor protein and the small signal change on ligand binding. Recently there have been reports of the kinetics of binding of fluorescent analogues of acetylcholine (Jürss et al., 1979; Heidmann & Changeux, 1979). These analogues have been shown to be agonists at the neuromuscular junction, but this method suffers from the disadvantage that ambiguity in the interpretation of the kinetic signals may arise from extrapolation of the effects of these compounds to describe the behavior of well-characterized agonists such as acetylcholine and Carb. Extrinsic fluorescence probes such as quinacrine (Grunhagen & Changeux, 1976; Grunhagen et al., 1976, 1977) and ethidium (Schimerlik et al., 1979; Quast et al., 1978, 1979) have also been used to monitor the interaction of agonists and AcChR-enriched membrane fragments. However, quinacrine acts as a local anesthetic (Grunhagen & Changeux, 1976) and thus itself affects the binding of agonists. In addition the possibility of uptake and dissociation of noncovalently bound probes during the course of an experiment as a result of ligand-induced conformational changes cannot be discounted (Schimerlik et al., 1979).

In this communication we describe an alternative method for monitoring agonist binding to membrane-bound AcChR from *Torpedo californica*. This approach makes use of ligand binding induced fluorescence changes of a probe covalently bound to the receptor. Nicotinic AcChR's are known to contain a disulfide bond in the vicinity of an agonist or antagonist binding site (Karlin, 1969) which, after reduction, can be readily alkylated by affinity reagents such as MBTA (Weill et al., 1974) and the agonist 2-bromoacetylcholine (Chang et al., 1977; Damle et al., 1978; Moore & Raftery, 1979a). This disulfide is therefore a convenient target for attack by a sulfydryl selective alkylating reagent. The fluorescent probe we have used for this purpose is 5-(iodoacetamido)salicylic acid (IAS) which has previously been used in fluorescence energy transfer studies of rhodopsin (Wu & Stryer, 1972).

We have measured the equilibrium binding properties of the specifically modified receptor and also the rapid kinetics of Carb binding. The results obtained are consistent with a more generalized form of a model previously proposed for agonist binding by Quast et al. (1978, 1979).

Experimental Procedures

Materials. *Torpedo californica* was obtained locally. Lyophilized venom of *Bungarus multicinctus*, Carb, and DTT were from Sigma Chemical Co. IAS was purchased from Molecular Probes, Inc. [^{3}H]Bromoacetylcholine was a generous gift from H.-P. Moore and [^{3}H]Carb from Dr. Y. Chao. All other materials were obtained from commercial sources.

Methods. Membrane fragments enriched in AcChR were prepared as previously described (Elliott et al., 1980). The concentration of α-BuTx binding sites was estimated by the disk assay method of Schmidt & Raftery (1973) with [^{125}I]-α-BuTx prepared as described by Blanchard et al. (1979) from lyophilized venom purified by the procedure of Clark et al. (1972). Protein concentration was determined by the method of Lowry et al. (1951). The ability of the AcChR to undergo an agonist-induced conformational change leading to higher affinity for agonists was measured as described by

† From the Church Laboratory of Chemical Biology, Division of Chemistry and Chemical Engineering, California Institute of Technology, Pasadena, California 91125. *Received February 19, 1980; revised manuscript received July 3, 1980.* Contribution No. 6176. Supported by U.S. Public Health Service Grant NS-10294 and by a grant from the Muscular Dystrophy Association of America.

[1] Abbreviations used: AcCh, acetylcholine; AcChR, acetylcholine receptor; α-BuTx, α-bungarotoxin; Carb, carbamylcholine; DTT, dithiothreitol; IAS, 5-(iodoacetamido)salicylic acid; MBTA, [4-(*N*-maleimido)benzyl]trimethylammonium iodide.

0006-2960/80/0419-5645$01.00/0

Lee et al. (1977) and Quast et al. (1978).

Covalent modification of AcChR-enriched membrane fragments by IAS was carried out as follows. Membrane fragments were diluted to a concentration of 1.0–1.5 μM in α-BuTx binding sites in Ca^{2+}-free Hepes Ringers (20 mM Hepes, 250 mM NaCl, 5 mM KCl, 2 mM $MgCl_2$, and 0.02% NaN_3, pH 7.4) which had been flushed with argon. DTT was added to a final concentration of 50 μM and reduction was allowed to proceed for 1 h at 4 °C. IAS was added from a stock concentration of 25 mM in 200 mM Tris, pH 8.5, to give a final concentration of 150–250 μM. The reaction mixture was shielded from light and, after adjustment of its pH to 7.5, was stirred for 2 h at 4 °C. The mixture was then diluted with the same buffer and centrifuged at 30 000 rpm for 45 min in a Beckman Type 35 rotor. The pellet was resuspended in a large volume of buffer and centrifuged as before. Final resuspension was in Ca^{2+}-free Ringers to give a final concentration of ~10 μM in α-BuTx binding sites. Covalent and reversible binding of bromoacetylcholine were carried out by using the procedures of Moore & Raftery (1979a).

All equilibrium and kinetic experiments were carried out with Hepes Ringers containing 4 mM $CaCl_2$. For measurements of the binding of [^{3}H]Carb, membrane fragments were equilibrated with various concentrations of radioactive ligand in a final volume of 1.5 mL for 30 min at room temperature. Duplicate 250-μL samples were withdrawn for liquid scintillation counting before and after the membrane fragments were pelleted for 15 min in an Eppendorf microfuge. Samples were counted in 8 mL of Aquasol-2 in a Packard Tricarb scintillation counter optimized for tritium. The concentration of bound ligand was calculated from the difference of total and free concentrations. Nonspecific binding of Carb was estimated from parallel experiments in which an excess of nonradioactive Carb was included in the incubation mixture. In most experiments the nonspecific component was sufficiently low to be neglected (<2% of bound).

Fluorescence spectra were recorded on a Perkin-Elmer MPF-4 spectrofluorimeter thermostated at 25 ± 1 °C. The equilibrium dissociation constant for the Carb-IAS-labeled receptor complex was obtained from a fluorescence titration using excitation and emission wavelengths of 282 ± 4 nm and 430 ± 4 nm, respectively. Five-microliter aliquots of Carb solution were added to 3 mL of membrane fragments in a 1-cm^2 cuvette. Equilibrium fluorescence measurements were recorded 5 min after ligand addition. In order to minimize photolytic reactions, samples were shielded from the light source between measurements. Small corrections for nonspecific effects were made by using the results of a parallel titration of IAS-labeled AcChR which had been preequilibrated with α-BuTx. Dissociation constants were calculated by a nonlinear regression method as described below.

Kinetic data were obtained by using a Durrum D-110 stopped-flow instrument equipped with a 75-W xenon lamp and operating in the fluorescence mode. Excitation was at 290 nm, and a UV bandpass filter (Corning 754) was used to eliminate stray light above 350 nm. Fluorescence emission was monitored by using a Corning 0-52 filter (50% transmission at 360 nm). The final concentration of membrane fragments after mixing was typically 0.5 μM in α-BuTx sites, and the temperature was maintained at 25 ± 1 °C. The amplified photomultiplier output was collected by using a Biomation model 805 transient recorder connected to a Digital Equipment Corporation MINC computer and a Tektronix 5103N storage oscilloscope, the latter being used only for visual monitoring of the data.

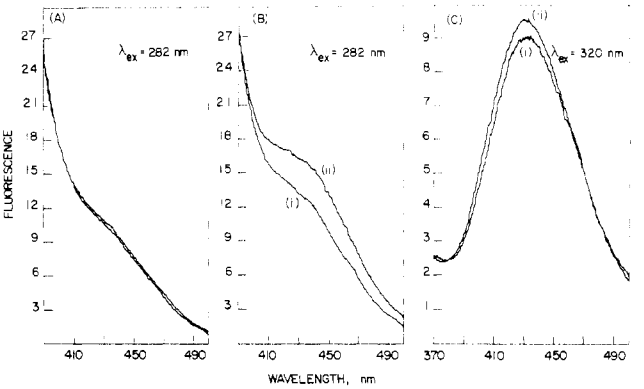

FIGURE 1: Fluorescence emission spectra of IAS-labeled membrane fragments. The AcChR concentration was 0.5 μM in α-BuTx binding sites, and spectra were recorded (i) either in the absence of (ii) or in the presence of 10 μM Carb. (A) Spectra of AcChR-enriched membrane fragments which were reacted with 150 μM IAS without prior reduction of the AcChR by DTT. (B) Energy transfer and (C) direct excitation spectra of labeled membrane fragments which were prepared as described in the text by reduction with 50 μM DTT followed by alkylation with 150 μM IAS.

All fluorescence data were analyzed by a nonlinear regression method using BASIC programs written for the MINC computer. This method uses the algorithm of Marquardt (1963) and was adapted from Bevington (1969). For each trace, both the raw data and the curve obtained by using the parameters derived from the fitting procedure were plotted on a Hewlett-Packard 7004B X-Y recorder to aid in the assessment of the fit of the data to the chosen experimental model. Typically 128 evenly spaced points of the 2048 collected for each trace were used in data analysis.

Kinetic data were analyzed by using either a single exponential equation

$$F(t) = A_0 + A_1[\exp(-k_1 t)] + k_0 t$$

or a sum of two exponentials

$$F(t) = A_0 + A_1[\exp(-k_1 t)] + A_2[\exp(-k_2 t)] + k_0 t$$

where $F(t)$ is the observed fluorescence at time t, A_0 is the equilibrium fluorescence level, A_1 and A_2 are the amplitudes of the two processes, and k_1 and k_2 are the corresponding rate constants. The term $k_0 t$ was included to correct for the component due to photolysis which was linear with time.

Fluorescence titration data were fitted to a simple binding curve and the kinetic parameters for each phase were fitted to the appropriate equations derived for the mechanism considered.

Results

Fluorescence Properties of IAS Modified Membrane Fragments. When IAS-labeled membrane fragments were excited at 320 nm, the excitation maximum of free IAS, maximum fluorescence emission was observed at 430 nm as shown in Figure 1C. Similar fluorescence emission was found when excitation was via energy transfer from the protein at 282 nm although this spectrum was complicated by the light scattering of the membrane fragments (Figure 1B). Addition of 10 μM Carb led to an enhancement of the fluorescence of bound IAS showing that the probe was sensitive to agonist binding. The observed increase in fluorescence was greater when excitation was at 282 nm, suggesting that the probe was indeed associated with the protein component of the membrane-bound receptor (Figure 1).

Figure 1A shows the fluorescence spectrum of membrane fragments which were not reduced with DTT prior to reaction

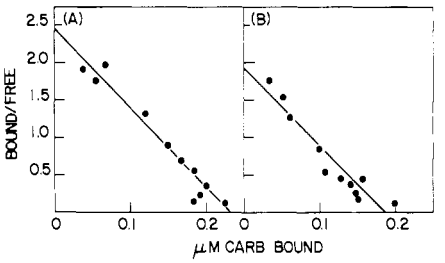

FIGURE 2: Scatchard plots of [^{3}H]Carb binding to AcChR-enriched membrane fragments. (A) [^{3}H]Carb binding to control membrane fragments. The AcChR concentration was 0.25 μM in α-BuTx sites. A linear least-squares fit to the data gave values of 93 ± 7 nM for the K_d and 0.23 ± 0.02 μM for the concentration of high-affinity Carb binding sites. (B) [^{3}H]Carb binding to IAS labeled membrane fragments. AcChR concentration was the same as in (A), and data fitting gave values of 94 ± 11 nM for the K_d and 0.18 ± 0.02 μM for the concentration of Carb binding sites.

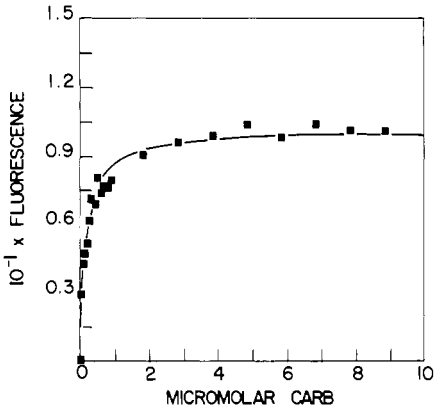

FIGURE 3: Fluorescence titration of IAS-labeled membrane fragments by Carb. Small volumes of Carb solution were added to 3 mL of labeled receptor, and the fluorescence enhancement (in arbitrary units) was measured with excitation and emission wavelengths of 282 and 430 nm, respectively. The concentration of Carb binding sites (0.37 μM) was estimated from the results of centrifugation assays by using radioactive Carb (Figure 2). The data were fitted to a simple binding equation, $F = F_0 L_f/(K_d + L_f)$, where F is the observed fluorescence, F_0 is the equilibrium fluorescence, and L_f is the free ligand concentration. The solid line was calculated from the best fit parameters, K_d = 171 ± 34 nM and F_0 = 10.1 ± 0.4.

with IAS. Considerable nonspecific labeling is apparent, indicating the existence of free sulfhydryl groups in the membranes even though they had been prepared in the presence of excess $IAcNH_2$ (Elliott et al., 1980). These groups were not significantly protected from IAS modification by further treatment with iodoacetamide, a result which may be due to differing reactivities of the two alkylating agents. However, membrane fragments which had been labeled without DTT reduction did not show a fluorescence enhancement on addition of Carb. It can therefore be concluded that the Carb-induced fluorescence change was not due to IAS modification of free sulfhydryl groups present in the nonreduced membrane preparations.

Extent of IAS Labeling. It has been shown that after reduction of the AcChR molecule by DTT it is readily alkylated by the agonist bromoacetylcholine (Moore & Raftery, 1979a). It seems likely in view of the relatively large signal change occurring on Carb binding to the IAS-modified receptor that the disulfide which is specifically modified by IAS is also in the vicinity of the agonist binding site. An attempt to assess the extent of labeling of this disulfide has therefore been made, assuming competitivity between IAS and bromoacetylcholine. Following inhibition of the acetylcholinesterase activity by addition of diethyl nitrophenyl phosphate to the membrane preparations, control and IAS-membrane fragments were reduced with 40 μM DTT prior to reaction with excess [^{3}H]bromoacetylcholine as described by Moore & Raftery (1979a). The extent of IAS labeling was estimated from the difference in bromoacetylcholine covalently bound to modified and control membrane preparations. For this particular preparation where 150 μM IAS was used in the modification procedure, the extent of labeling was 54% of the bromoacetylcholine sites. It is clear from recent results that an increased fluorescence change on Carb addition, and thus a higher degree of labeling can be obtained by increasing the concentration of IAS used in the treatment to 250 μM and by more careful control of the DTT reduction step.

Reversible binding of bromoacetylcholine was measured by centrifugation assay. This experiment revealed that IAS treatment did not alter the ability of membrane-bound AcChR to bind this agonist reversibly, suggesting that IAS presence did not significantly affect the reversible binding of agonists.

Effect of IAS Modification on the Ligand Binding Properties of the AcChR. Measurement of a α-BuTx binding activity and protein concentration of membrane fragments before and after treatment with IAS have shown that modification did not affect the specific activity of the membrane preparation. IAS-labeled membrane fragments retained the ability to undergo a change to a state of higher affinity for agonists on exposure to low concentrations of Carb.

The dissociation constant for Carb binding and number of binding sites were measured by a centrifugation assay with [^{3}H]Carb. The results shown in Figure 2 suggest that IAS treatment did not alter either the K_d for Carb binding (~100 nM) or the stoichiometry of Carb and α-BuTx binding sites. No evidence for heterogeneity of binding sites was found. These binding assays have been repeated with several different membrane preparations, and similar results were obtained from each experiment. On a few occasions, a small reduction in the apparent number of Carb sites (to about 75% of the control) was observed after treatment. This may be attributable to partial blocking of the receptor in a low affinity form for Carb as a result of reduction and alkylation as described by Moore & Raftery (1979b).

The results of a fluorescent titration of IAS-labeled membrane fragments by Carb are shown in Figure 3. A nonlinear regression fit to this data after correction for bound ligand gave a K_d value of 171 ± 34 nM. This is in very good agreement with the value obtained for the same preparation by centrifugation assay with radioactive ligand (shown in Figure 2) and indicates that the fluorescence changes of bound IAS is a sensitive and accurate monitor of Carb binding.

Qualitative Description of the Kinetics of Carb Binding to IAS-Labeled Membrane Fragments. The reaction traces obtained when Carb was rapidly mixed with labeled receptor were complex and could be resolved into four distinct components. Fortunately these four phases were fairly well separated in rate which enabled kinetic parameters for each phase to be obtained by careful control of the timing used in data collection (Figure 4).

The fastest phase (phase 1, Figure 4A) having an apparent rate of ~30 s^{-1} was sufficiently well-separated temporally that it could be analyzed in isolation and was fitted to a single exponential equation. The three slower phases were monitored over several time courses by varying the sampling rate for data collection as shown in Figure 4B,C. Most of these reaction traces were fitted to a sum of two exponentials. For further analysis and mechanism fitting, parameters for any phase which had been obtained from traces in which the time scale

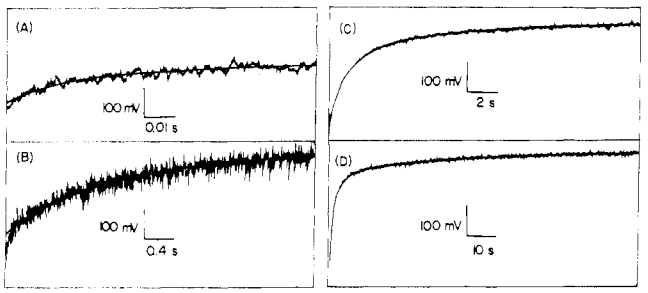

FIGURE 4: Kinetics of Carb binding to IAS-labeled membrane fragments. Stopped-flow traces were obtained by rapid mixing of 0.5 μM AcChR (in α-BuTx sites) and 7.5 μM Carb (final concentrations after mixing). The solid lines were calculated from the kinetic parameters given below which were obtained from nonlinear regression fitting of the data to either a single exponential or to a sum of two exponentials as described under Methods. Parameters given in parentheses were not sufficiently reliable for use in further analysis (see text). (A) Fastest phase (phase 1): A_1 = 91 mV, k_1 = 54.0 s^{-1}. (B) Fast time scale: A_1 = 206 mV, k_1 = 0.96 s^{-1}. (C) Intermediate time scale: (A_1 = 173 mV), (k_1 = 125 s^{-1}), A_2 = 135 mV, k_2 = 0.29 s^{-1}. (D) Slow time scale: (A_1 = 266 mV), (k_1 = 0.69 s^{-1}), A_2 = 73 mV, k_2 = 0.076 s^{-1}.

of the experiment exceeded the half-time of that phase by a factor of less than 2.5 or more than 25 were rejected. In this way reliable data could be obtained for each of the three slower phases over a wide range of ligand concentrations.

The kinetic behavior of Carb binding to several membrane preparations has been examined, and little preparation dependence has been observed. In addition, neither the age of the preparation nor the exposure of the membrane fragments to calcium during the course of an experiment noticeably perturbed the observed kinetics (cf. Quast et al., 1979).

Specificity of the Fluorescence Signal Change. When α-BuTx was mixed with IAS-labeled membrane fragments, the major component of the reaction trace was a linear decrease in flurescence. The experiment illustrated in Figure 5A showed that this decrease was due to photolytic reactions. At the points marked, the excitation slit was closed, thus shielding the reaction mixture from the light source. When the slit was reopened after a short time interval, the fluorescence level returned to that prior to slit closure. This showed that the signal decrease occurred only under illumination and was therefore due to photolysis. The presence of α-BuTx appeared to increase the rate of photolysis, possibly due to an increase in absorbance of the probe as a result of energy transfer from the toxin. In the absence of α-BuTx, the light-dependent effects were much reduced, and when membrane fragments were mixed with Ringers alone, there was no evidence of the nonlinearity shown in Figure 5A which was observed immediately after mixing.

Figure 5B shows the kinetic traces recorded when IAS-labeled membrane fragments which had been preequilibrated with excess α-BuTx were rapidly mixed with Ringers and with 10 μM Carb. The difference between these two curves is plotted in the upper panel of this Figure and shows that the Carb-induced fluorescence enhancement was completely blocked by prior binding of α-BuTx to the receptor. Similar results were obtained over all time scales, showing that the signal observed on binding of Carb was due to IAS specifically bound to the AcChR molecule.

Effect of Carb Concentration on Binding Kinetics. The fastest phase observed (Figure 4A) was apparent only at low ligand concentration, and its rate (30–40 s^{-1}) showed little concentration dependence. However, its amplitude, after an initial increase, began to decrease at concentrations of Carb above 2 μM. This phase could therefore be examined over

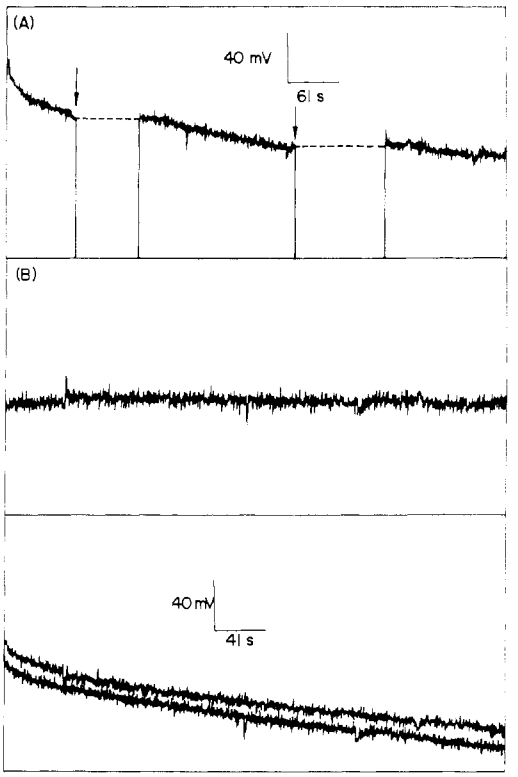

FIGURE 5: Effect of α-BuTx on fluorescence of IAS-labeled membrane fragments. (A) Kinetic trace recorded when 2 μM α-BuTx was mixed with 0.5 μM AcChR (final concentrations). At the points marked with an arrow, the excitation slit was closed thus shielding the reaction mixture from the light source. After a short time period (>1 min), the slit was opened and signal recording was resumed. The decrease in fluorescence occurred only under illumination and was therefore due to photolysis. (B) The lower panel shows the change in fluorescence when 0.5 μM labeled AcChR which had been preequilibrated with 1.0 μM α-BuTx for 60 min was mixed with Ringers solution (upper trace) or with 10 μM Carb (lower trace). The difference between these traces is illustrated in the upper panel of this figure and shows that preincubation of the receptor with α-BuTx completely abolished the Carb-induced fluorescence enhancement.

only a small concentration range. As a result, reliable estimates for the kinetic parameters of this phase are difficult to obtain. For this reason, this phase has not, at this stage, been included in the mechanism proposed in the next section. This will be further dealt with under Discussion.

Figure 6 shows the effect of Carb concentration on the rates and amplitudes of the other three phases. The rates of both the fast (Figure 6A) and intermediate phase (Figure 6B) increased with increasing ligand concentration until reaching a saturating level. The kinetics of the slow phase (Figure 6C) were apparently more complicated in that its rate and amplitude decreased after a maximum level at approximately 2–3 μM was reached.

Kinetic Mechanism for Carb Binding. The ligand concentration dependencies of the kinetic parameters describing the intermediate and slow phases bear a striking similarity to the two phases observed when Carb binding to AcChR-enriched membranes were monitored by changes in the fluorescence of the noncovalently bound probe, ethidium (Quast et al., 1978, 1979). There are few simple mechanisms which can explain the disappearance of the slow phase at high ligand concentrations. Quast et al. (1979) discussed many models which did not satisfactorily account for the observed kinetic data. We have considered similar and additional mechanisms extended to account for the third (fast) exponential and have found that the *simplest* mechanism which is consistent with

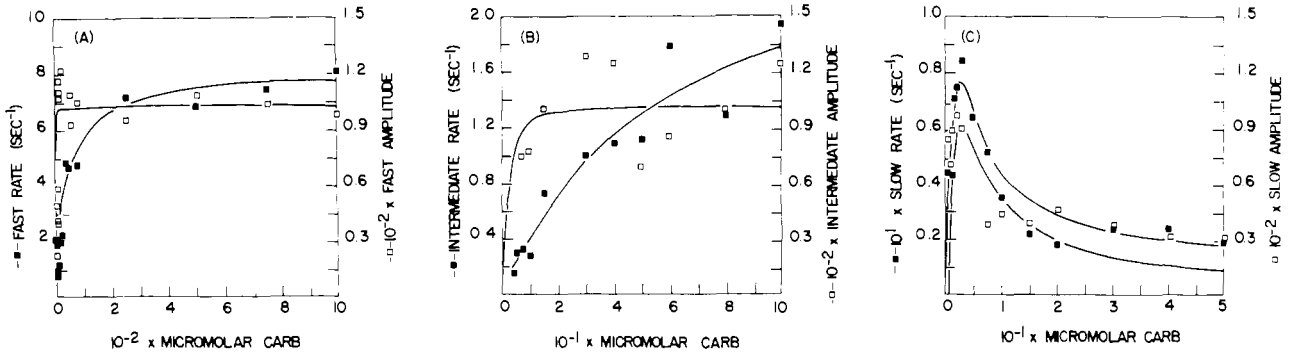

FIGURE 6: Effect of Carb concentration on kinetics of binding to IAS-labeled AcChR. The rates (■) and amplitudes (□) of the fast, intermediate, and slow phases are plotted as a function of Carb concentration. Solid lines are those obtained from a fit of the data to the appropriate equations describing mechanism 1 (see text). The kinetic parameters obtained for each phase are given below and in Table I. (A) Fast phase: (rate) $k_{-2}K_4 = 46.6\ \mu M\ s^{-1}$, $K_4 = 50.8\ \mu M$, $k_2 = 8.1\ s^{-1}$, $K_1 = 50.8\ \mu M$; (amplitude) $QR_0 = 102$ (not fitted). (B) Intermediate phase: (rate) $k_{-5} = 0.044\ s^{-1}$, $K_1K_2 = 5.74\ \mu M$, $K_1K_2K_4 = 291.6\ \mu M^2$, $k_5/K_1K_2K_4 = 0.0092\ \mu M^{-2}\ s^{-1}$; (amplitude) $QR_0 = 104$. (C) Slow phase: (rate) $k_{-3} = 0.008\ s^{-1}$, $k_3/K_1K_2 = 0.0723\ \mu M^{-1}\ s^{-1}$, $K_1K_2K_4K_5 = 5.05\ \mu M^2$; (amplitude) $QR_0 = 85$.

the ligand concentration dependencies of all three phases (omitting the fastest phase as described above) is

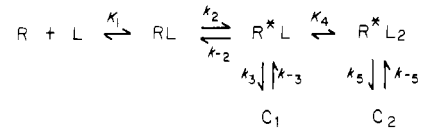

(1)

in which K_1 and K_4 are dissociation constants of the two receptor ligand complexes, RL and R*L_2, and can be considered as fast preequilibrations to the subsequent isomerization reactions. This mechanism is clearly very similar to that proposed by Quast et al. (1978, 1979) but is complicated by the inclusion of step 2 (RL ⇌ R*L) which corresponds to the fast phase observed. In this mechanism, the intermediate phase arises from C_2 formation and the slow phase from formation of C_1. According to this scheme, the binding of a second ligand to R*L at high ligand concentrations drives the equilibrium in favor of C_2 formation, and therefore in this concentration range, the slow phase due to step 3 is reduced.

The effect of ligand concentration on the kinetic parameters of each phase can be calculated by an extension of the procedure described by Quast et al. (1979) which is summarized in an appendix (see paragraph at end of paper regarding supplementary material). The proposed mechanism gives rise to three relaxation times which are designated as λ for each phase and show the following ligand concentration dependencies:

(a) fast phase (Figure 6A)

$$\lambda_F = \frac{k_{-2}K_4}{K_4 + L} + \frac{k_2 L}{K_1 + L} \tag{2}$$

(b) intermediate phase (Figure 6B)

$$\lambda_I = k_{-5} + \frac{k_5\left(\frac{L^2}{K_1K_2K_4}\right)}{1 + \frac{L}{K_1K_2} + \frac{L^2}{K_1K_2K_4}} \tag{3}$$

(c) slow phase (Figure 6C)

$$\lambda_S = k_{-3} + \frac{k_3\left(\frac{L}{K_1K_2}\right)}{1 + \frac{L}{K_1K_2} + \frac{L^2}{K_1K_2K_4K_5}} \tag{4}$$

The rate of the slow phase reaches a maximum value at a ligand concentration, $L_{max} \approx (K_1K_2K_4K_5)^{1/2}$.

Table I: Kinetic Parameters for Carb Binding to IAS-Labeled AcChR and Comparison With Data of Quast et al. (1979)

(A) parameters derived from mechanism 1		(B) data from Table I, row 1, of Quast et al. (1979)	
parameter	value	corresponding parameter	value
K_1	50.8 μM		
k_2	8.1 s^{-1}		
k_{-2}	0.9 s^{-1}		
K_4	50.8 μM	K_4'	58.0 μM
k_5	2.7 s^{-1}	k_2'	2.3 s^{-1}
k_{-5}	0.04 s^{-1}	k_{-2}'	0.10 s^{-1}
k_3	0.42 s^{-1}	k_1'	0.03 s^{-1}
k_{-3}	0.008 s^{-1}	k_{-1}'	0.002 s^{-1}
K_1K_2	5.7 μM	K_1'	1.3 μM
$K_1K_2K_3$	0.12 μM	K_1K_1'	0.10 μM
K_4K_5/K_3	42.0 μM	K_{eff}	30.0 μM
$K_1K_2K_4K_5$	5.0 μM^2	$K_1K_2K_2'$	2.6 μM^2

Nonlinear regression procedures without constraint were used to fit the rates of each phase to the derived equations. The best fit parameters obtained from different phases showed a high level of consistency, and an iterative procedure rapidly converged to a set of parameters which described the behavior of each phase with precision. The kinetic constants thus obtained are given in Table I where they are compared with the corresponding values obtained by Quast et al. (1979).

The amplitude data were also consistent with mechanism 1 although these data themselves showed considerable scatter due to difficulties inherent in obtaining accurate amplitude data when three phases coexist. The experimental data require that a quantum-yield change occurs in each of the three isomerization steps. Furthermore, the maximum amplitudes of the three phases are similar, suggesting that the three quantum-yield changes are equal, a suggestion borne out by data fitting to the proposed model.

At equilibrium the total amplitude is approximately equal to the concentrations of C_1 and C_2 since the concentrations of all other species will be small. The total amplitude can therefore be approximated by the relationship

$$A_T \approx 2QR_0\left[\frac{\frac{L}{K_1K_2K_3} + \frac{L^2}{K_1K_2K_4K_5}}{1 + \frac{L}{K_1K_2K_3} + \frac{L^2}{K_1K_2K_4K_5}}\right] \tag{5}$$

(neglecting the terms L/K_1K_2 and $L/K_1K_2K_4$ in the denominator since these are small) in which Q is the quantum-yield

change. The factor of 2 is introduced because of the signal change occurring in the fast phase (i.e., formation of R*L) which is a prerequisite for both C_1 and C_2 formation.

The concentration dependencies of the intermediate and slow phases are discussed in the supplementary material and can be approximated by

$$A_I \approx Q\left(\frac{\lambda_s}{k_{-5}}\bar{C}_1 + \frac{\lambda_s}{k_{-3}}\bar{C}_2\right) \quad (6)$$

for the intermediate phase and

$$A_s \approx Q\left[\left(1-\frac{\lambda_s}{k_{-5}}\right)\bar{C}_1 + \left(1-\frac{\lambda_s}{k_{-3}}\right)\bar{C}_2\right] \quad (7)$$

for the slow phase (bars denote concentrations at equilibrium).

The fits of the data to these equations are shown in Figure 6. The values obtained for Q from independent fitting of the intermediate and slow phase data were 104 and 85 (arbitrary units), respectively, which are in good agreement with the estimate of 109 obtained from the total amplitude (data not shown). The fast phase was not fitted directly (Figure 6A) but could be fitted with precision by using the values obtained from the other three fits.

Discussion

A reactive disulfide bond near an agonist binding site of the nicotinic AcChR (Karlin, 1969) can be readily reduced and alkylated by certain affinity reagents, both antagonists (Weill et al., 1974) or an agonist (Moore & Raftery, 1979a). This suggested its usefulness as a target for alkylation by a sulfhydryl-specific reagent whose fluorescence could be used to monitor the interactions of agonists and the receptor molecule. IAS has proved to be an ideal probe for this purpose since its ready solubility in water reduces the possibility of noncovalent interaction with membrane lipids and facilitates the alkylation reaction. More importantly, the fluorescence of the probe is sensitive to environmental changes, and, because of its small size, it does not appear to seriously perturb the agonist binding properties of the receptor.

Equilibrium binding assays with radioactive Carb have shown that for most preparations neither the K_d of the complex nor the stoichiometry of Carb and toxin binding was altered as a result of IAS modification. In these preparations, a change to a state having high affinity for agonists could be induced by exposure to Carb, leading to an overall K_d for Carb of $\sim$100 nM. In a few experiments, however, a slight decrease in the apparent number of Carb sites was found after treatment. Moore & Raftery (1979b) have reported that reduction of the membrane-bound receptor with 1 mM DTT followed by iodoacetamide alkylation resulted in a blocking of the receptor in a form having low affinity for agonists. Such membrane preparations have a K_d for Carb binding close to 30 μM. A possible explanation for the slight loss of binding sites during IAS modification is therefore that, in spite of the low DTT concentration used (50 μM), partial blocking of the receptor in the low affinity form had occurred. Under the experimental conditions of the binding assays, binding of Carb to these low affinity sites would not be apparent, and thus no biphasicity of the Scatchard plots would be expected.

Reaction of AcChR with IAS inhibited the covalent labeling of the receptor by the alkylating agonist bromoacetylcholine. This strongly suggests that the modified disulfide bond which is responsible for the fluorescence enhancement induced by the binding of Carb is located near the agonist binding site. Reversible binding of bromoacetylcholine was not noticeably affected by receptor modification, and this is further evidence that the agonist and IAS can coexist at the binding site.

The fluorescence properties of bound IAS have been shown to be sensitive to the interaction of Carb and the receptor. In addition, the signal change observed was specific since it was completely abolished by preincubation of the receptor with α-BuTx. The consistency of the K_d values obtained from the radioactive ligand binding assays (Figure 2) and from the fluorescence titration data (Figure 3) showed that the Carb induced fluorescence enhancement is an accurate measure of complex formation.

The fluorescence enhancement accompanying Carb binding to IAS-labeled membrane fragments could be resolved into four distinct components each of which could be fitted with precision to a single exponential (Figure 4). The rates of the three slower phases were sufficiently well separated that reliable measurements of their kinetic parameters were obtained over a wide range of ligand concentrations (Figure 6). A model (mechanism 1) has been proposed which is consistent with the behavior of these phases. This mechanism is necessarily complex and includes two ligand binding steps and three conformational changes each of which is accompanied by a change in the quantum yield of bound IAS. The overall equilibrium constant for the binding of the first ligand derived for this mechanism ($K_1K_2K_3$) is 116 nM (Table I), which is in excellent agreement with that of 93 nM measured by centrifugation assay of Carb binding to the high-affinity site (Figure 2). An effective dissociation constant for the second ligand binding can be approximated by K_4K_5/K_3 (see Quast et al., 1979), giving a value of 42 μM (Table I). Thus there is a significant difference in the affinities of the two binding sites, and, as a consequence of the experimental conditions used, binding of this second ligand would not be expected to contribute to the equilibrium binding assays shown in Figures 2 and 3.

The similarity of the mechanism discussed here and that proposed by Quast et al. (1978, 1979) to account for agonist binding behavior observed by changes in ethidium fluorescence is remarkable. Undoubtedly both IAS and ethidium to some extent themselves perturb the system under study. However, the finding that two entirely different approaches indicate agonist binding behavior which is consistent with the same general mechanism is clearly important.

The major difference between the two mechanisms is that here the appearance of the fast phase necessitates the inclusion of an additional isomerization step immediately following the binding of the first ligand (step 2; mechanism 1). Omission of this phase would not lead to a degeneration of mechanism 1 to that proposed by Quast et al. (1978, 1979). In the absence of the fast step, the equilibrium constant for the first ligand binding would be given by K_1K_3 which has a value of 1 μM (from Table I). This is clearly inconsistent with both the equilibrium binding data presented here and the value of 0.10 μM reported by Quast et al. (1979; Table I). Mechanism 1 should not therefore be considered as an extension of the previously proposed model but rather as a more complete form of that mechanism. It is possible that when ethidium was used to monitor agonist binding kinetics step 2 of mechanism 1 was a mute step in that no change in ethidium fluorescence occurred in the formation of R*L. The binding of the first ligand and isomerization of the initial complex to R*L would then approximate a fast equilibrium reaction and would not therefore seriously affect the kinetic analysis of the two slower phases.

Comparisons of the parameters obtained from fitting mechanism 1 with those reported by Quast et al. (1979) in-

dicate some discrepancies in the values describing the slow phase, which we find to be an order of magnitude higher than those previously reported (Table I). It should be noted, however, that these constants affect only the magnitude of the maximum rate of the slow phase occurring at low ligand concentration (Figure 6C) and thus can be varied without substantial effect on the mechanism. A more significant variation in the kinetics observed in the present study from those described by Quast et al. (1978, 1979) is that at high ligand concentration we see no evidence for the binding of additional ligand molecules. Despite these differences, the similarity of the kinetic behavior observed by these two independent approaches is perhaps surprising since the membrane preparations used here consistently showed a stoichiometry of one high-affinity Carb site per α-BuTx site, whereas the preparations used by Quast et al. (1979) had a ratio of Carb to toxin sites of 0.5. A possible interpretation for this is that only one of the two Carb sites contains a disulfide bond capable of modification by IAS. In such a case, the fluorescence of bound IAS would reflect the kinetics of Carb binding to only half of the available sites. However, the linearity of the Scatchard plots shown in Figure 2 indicates one homogeneous class of noninteracting Carb binding sites. It would therefore be possible that, even though only half of the binding sites had been labeled by IAS, the signal change observed on binding of Carb would be an accurate reflection of the behavior of the receptor as a whole.

Despite its complexity, mechanism 1 cannot account for the appearance of a faster phase (Figure 4A) which was observed at low ligand concentrations and had a rate of 30–40 s^{-1}. As was described under Experimental Procedures, this phase was necessarily neglected in the discussion of the proposed mechanism because of the unreliability of the kinetic constants obtained for this phase. As a consequence of this omission, mechanism 1 must be considered as only a simplified model for Carb binding. It is clear from the results that phase 1 cannot be attributed to a ligand binding step since its rate does not significantly increase with ligand concentration, as would be expected of a bimolecular reaction. In addition, the amplitude of this phase seems to parallel that of the slow phase, and this leads to the tentative proposal that these two phases are closely related. One possibility is that phase 1 arises from formation of an intermediate in the $R^*L \rightleftharpoons C_1$ conformational change. Such a scheme is qualitatively consistent with the data, and, although it changes the interpretation of some kinetic parameters, it does not affect the form of the concentration dependence of the other phases. However, assignment of this phase must await more reliable evidence which may be obtained from studies of other cholinergic effectors.

Heidmann & Changeux (1979) have recently reported their results from a study of the kinetics of the binding of a fluorescent agonist (dansyl-C_6-choline) to membrane-bound AcChR from *Torpedo marmorata*. They have interpreted their results in terms of a model in which there are two preexisting states of the receptor which are interconvertible. The observed kinetics of Carb binding to IAS-labeled membrane fragments are quite different from those seen for dansyl-C_6-choline binding and are inconsistent with such a two-state mechanism.

In the absence of supporting evidence, it is difficult to correlate the kinetic behavior described here with the physiological responses of the receptor. However, the results require that at least two ligands must bind to the IAS-labeled receptor, which is consistent with electrophysiological studies which indicate that more than a single ligand binding is required to activate the ion channel in vivo. No attempt has been made here to ascribe any step to the opening of the channel in the membrane. It is hoped that further information obtained from examination of the effects of channel blockers such as histrionicotoxin or local anesthetics on agonists binding kinetics will aid in the interpretation of the kinetic data at the functional level of the receptor.

Acknowledgments

We thank Hsaio-Ping Moore for her help with the bromoacetylcholine labeling experiments. We are also grateful to John Racs for technical assistance and to Valerie Purvis for artwork and typing the manuscript.

Supplementary Material Available

An appendix giving the mathematical treatment of mechanism 1, including the fast relaxation, step 2 (4 pages). Ordering information is given on any current masthead page.

References

Barrantes, F. J. (1976) *Biochem. Biophys. Res. Commun. 72*, 479–488.

Bevington, P. R. (1969) *Data Reduction and Error Analysis for the Physical Sciences*, McGraw-Hill, New York.

Blanchard, S. G., Quast, U., Reed, K., Lee, T., Schimerlik, M. I., Vandlen, R., Claudio, T., Strader, C. D., Moore, H.-P. H., & Raftery, M. A. (1979) *Biochemistry 18*, 1875–1883.

Bonner, R., Barrantes, F. J., & Jovin, T. M. (1976) *Nature (London) 263*, 429–431.

Chang, R. S. L., Potter, L. T., & Smith, D. S. (1977) *Tissue Cell 9*, 623–628.

Clark, D. G., Macmurchie, D. D., Elliott, E., Wolcott, R. G., Landel, A. M., & Raftery, M. A. (1972) *Biochemistry 11*, 1663–1668.

Damle, V. N., McLaughlin, M., & Karlin, A. (1978) *Biochem. Biophys. Res. Commun. 84*, 845–851.

Elliott, J., Blanchard, S. G., Wu, W., Miller, J., Strader, C. D., Hartig, P., Moore, H.-P., Racs, J., & Raftery, M. A. (1980) *Biochem. J. 185*, 667–677.

Grünhagen, H. H., & Changeux, J.-P. (1976) *J. Mol. Biol. 106*, 479–516, 517–535.

Grünhagen, H. H., Iwatsubo, M., & Changeux, J.-P. (1976) *C.R. Hebd. Seances Acad. Sci., Ser. D 283*, 1105–1108.

Grünhagen, H. H., Iwatsubo, M., & Changeux, J.-P. (1977) *Eur. J. Biochem. 80*, 225–242.

Heidmann, T., & Changeux, J.-P. (1979) *Eur. J. Biochem. 94*, 255–279.

Jürss, R., Prinz, H., & Maelicke, A. (1979) *Proc. Natl. Acad. Sci. U.S.A. 76*, 1064–1068.

Karlin, A. (1969) *J. Gen. Physiol. 54*, 245S–264S.

Lee, T., Witzemann, V., Schimerlik, M. I., & Raftery, M. A. (1977) *Arch. Biochem. Biophys. 183*, 57–63.

Lowry, O. H., Rosenbrough, N. J., Farr, A., & Randall, R. J. (1951) *J. Biol. Chem. 193*, 265–275.

Marquardt, D. W. (1963) *J. Soc. Ind. Appl. Math. 11*, 431–441.

Moore, H.-P. H., & Raftery, M. A. (1979a) *Biochemistry 18*, 1862–1867.

Moore, H.-P. H., & Raftery, M. A. (1979b) *Biochemistry 18*, 1907–1911.

Quast, U., Schimerlik, M. I., & Raftery, M. A. (1978) *Biochem. Biophys. Res. Commun. 81*, 955–964.

Quast, U., Schimerlik, M. I., & Raftery, M. A. (1979) *Biochemistry 18*, 1891–1901.

Schimerlik, M. I., Quast, U., & Raftery, M. A. (1979) *Biochemistry 18*, 1884–1890.
Schmidt, J., & Raftery, M. A. (1973) *Anal. Biochem. 52*, 349–354.
Weill, C. L., McNamee, M. G., & Karlin, A. (1974) *Biochem. Biophys. Res. Commun. 61*, 997–1003.
Wu, C.-W., & Stryer, L. (1972) *Proc. Natl. Acad. Sci. U.S.A. 69*, 1104–1108.

Structural Analysis of Glycosphinoglipids by High-Resolution ^{1}H Nuclear Magnetic Resonance Spectroscopy†

Janusz Dabrowski,* Peter Hanfland, and Heinz Egge

ABSTRACT: The carbohydrate composition of eight glycosphingolipids–glucosylceramide, lactosylceramide, lacto-*N*-triaosylceramide, neolactotetraosylceramide, IV^{3}Galαneolactotetraosylceramide, globotriaosylceramide, globoside (P-antigen), and Forssman glycolipid (IV^{3}GalNAcα-GbOse$_4$Cer)—derived from different sources was analyzed by ^{1}H nuclear magnetic resonance at 360 MHz in dimethyl-d_6 sulfoxide as solvent. The resonances of all H-1 and H-2 protons as well as those of most of the H-3 and H-4, and of some H-5 protons, of the sugar rings were assigned with the aid of spin decoupling difference spectroscopy. They show regularities related to the type, anomeric configuration, site of glycosidic linkage, and sequence of the component sugars glucose, galactose, glucosamine, and galactosamine. These regularities are thus suited for elucidation of hitherto unknown structures of more complex glycosphingolipids.

Increasing knowledge of the biological functions of glycosphingolipids as compounds of cellular surfaces, particularly of their blood-group antigenicity (Hakomori & Kobata, 1974; Hanfland, 1975; Hanfland et al., 1978a; Koscielak et al., 1979; Watanabe et al., 1979), as well as of their role in cellular recognition, growth control, and malignant degeneration (Hakomori, 1975; Hanfland & Uhlenbruck, 1978) has promoted the development of microscale characterization methods; combined gas chromatography–mass spectrometry of partially methylated alditol acetates (Björndal et al., 1970; Stoffel & Hanfland, 1973; Stellner et al., 1973), direct-inlet mass spectrometry of permethylated glycolipids (Karlsson et al., 1974; Ledeen et al., 1974; Hanfland & Egge, 1976; Egge, 1978), and enzymatic degradation by specific glycosidases (Hakomori et al., 1971; Hanfland et al., 1978b) allow one to evaluate sugar linkage and sequence as well as anomeric configuration. However, regarding the tiny amount of material obtainable from some sources, its loss due to these destructive methods is a serious disadvantage. High-resolution ^{1}H NMR spectroscopy is a nondestructive method well suited for elucidation of complex structures. However, if the degree of complexity exceeds certain limits, the problem of overlapping multiplets must be solved. Although several recent investigations on oligosaccharides (Dorland et al., 1977) and glycosphingolipids (Martin-Lomas & Chapman, 1973; Falk et al., 1979) benefited by the enhanced spectral resolution of the high-field spectrometers now available, the source of information was still limited to signals which occurred outside of the bulk of overlapping resonances and could thus be found by inspection. In our work, we show that additional structural information can be obtained from signals extracted by means of spin-decoupling difference spectroscopy (SDDS;[1] Gibbons et al., 1975) from the originally uninterpretable signal agglomerates.

The glycosphingolipids **1**–**10** related to the Forssman glycolipid (IV^{3}GalNAcα-GbOse$_4$Cer) and the ceramide pentasaccharide IV^{3}GalαnLcOse$_4$Cer from rabbit erythrocytes with B-like blood group activity offer manifold combinations in which the sugars, their anomeric configuration, sequence, and the sites of glycosidic linkage are the variables. We demonstrate that some regularities concerning the chemical shifts of several of the sugar protons (Tables I–V) enable one to determine these variables.

Materials and Methods

Preparation of Glycosphingolipids. Glucosylceramide (**1**) obtained from IV^{3}Galα-nLcOse$_4$Cer (**10**) after repeated partial hydrolysis with 0.1 N HCl at 90 °C for 40 min was purified by preparative silica gel high-performance thin-layer chromatography with $CHCl_3$/MeOH/H_2O (75:16:2) as developing solvent (Hanfland, 1978).

Forssman glycolipid (**7**) was isolated from equine kidneys according to the procedures described for the glycosphingolipids B-I and B-II (Hanfland & Egli, 1975) and purified by preparative high-performance thin-layer chromatography (Hanfland, 1978). The identification as IV^3 GalNAcα-GbOse$_4$Cer (**7**) is based on sugar analysis (Hanfland et al., 1978b), analysis of the partially methylated alditolacetates (Stoffel & Hanfland, 1973), and two-dimensional immunodiffusion against *Dolichos biflorus* lectin.

Globotetraosylceramide from human erythrocyte membranes (**6**), globotriaosylceramide with both *n*-FA and α-hydroxy fatty acid (HFA) residues (**4**) and (**5**), and lactosylceramide, also with FA (**2**) and HFA (**3**) residues, from human plasma, as well as IV^{3}Galα-nLcOse$_4$Cer (**10**) from rabbit erythrocyte membranes were obtained by methods described earlier (Hanfland & Egli, 1975; Hanfland, 1978).

† From the Max-Planck-Institut für Medizinische Forschung, D-6900 Heidelberg, Germany (J.D.), the Institut für Experimentelle Hämatologie und Bluttransfusionswesen der Universität Bonn, D-5300 Bonn, Germany (P.H.), and the Physiologisch-Chemisches Institut der Universität Bonn, D-5300 Bonn, Germany (H.E.). *Received March 7, 1980.*

[1] Abbreviations used: FT NMR, Fourier-transform nuclear magnetic resonance; SDDS, spin-decoupling difference spectroscopy; FA and HFA, fatty acid and α-hydroxy fatty acid of the ceramide part; INDOR, internuclear double resonance; SPI, selective population inversion; SECSY, spin-echo correlated spectroscopy; Me_2SO, dimethyl sulfoxide.

0006-2960/80/0419-5652$01.00/0